INFERRING FUNCTIONAL CONNECTIVITY USING SPATIAL MODULATION MEASURES OF FMRI SIGNALS WITHIN BRAIN REGIONS OF INTEREST

Bernard Ng[1], Rafeef Abugharbieh[1], Martin J. McKeown[2]

[1] Department of Electrical and Computer Engineering,
[2] Department of Medicine (Neurology), Pacific Parkinson's Research Center,
University of British Columbia, Vancouver, BC, Canada, bernardn@ece.ubc.ca

ABSTRACT

We propose inferring functional connectivity between brain regions by examining the spatial modulation of the blood oxygen level dependent (BOLD) signals within brain regions of interest (ROIs). This is motivated by our previous work, where the spatial distribution of BOLD signals within an ROI was found to be modulated by task. Applying replicator dynamics to our proposed spatial feature time courses on real functional magnetic resonance imaging (fMRI) data detected task-related changes in the composition of the brain's functional networks, whereas using classical mean intensity features resulted in little changes being detected. Thus, our results suggest that intensity is not the only co-activating feature in fMRI data. Instead, spatial modulations may also be used for inferring functional connectivity.

Index Terms— fMRI, functional connectivity, spatial modulation, replicator dynamics, region of interest (ROI)

1. INTRODUCTION

In this work, we study the functional integration of the brain using functional magnetic resonance imaging (fMRI). Functional integration refers to the interactions between distinct spatial locations in the brain, and can be characterized in terms of functional and effective connectivity [1]. Functional connectivity corresponds to the "temporal correlations between spatially remote neurophysiological events", whereas effective connectivity is "the influence one neuronal system exerts over another" [1]. In the current study, we focus on examining functional connectivity for detecting task-related brain networks, which helps guide the selection of regions of interest (ROIs) that are sensible for subsequent effective connectivity analysis.

Functional connectivity can be examined at either the voxel or ROI level. At the voxel level, principal component analysis (PCA) or variants thereof is, by far, the most commonly used approach [2, 3]. PCA decomposes the fMRI signals into a set of orthogonal modes with the first mode corresponding to the most correlated set of voxels and subsequent modes relating to sets of voxels with decreasing degree of correlation. Voxel level approaches have been applied to study different functional brain properties such as resting state connectivity [4], but complications arise when group inferences are to be made due to inter-subject variability in brain shapes, brain sizes, and subject's orientation in the scanner. To generate voxel correspondence across subjects, each subject's brain has to be warped onto a common template, but warping is prone to mis-registration errors [5]. To avoid spatial warping, the alternative approach, as adopted in this paper, is to specify ROIs and examine statistical measures of regional activation.

Inferring functional connectivity between brain regions requires defining a feature to represent the response of each ROI. Traditionally, mean intensity time courses averaged over an ROI were used [6]. Such representation assumes that only the intensity of blood oxygen level dependent (BOLD) signals is modulated by task. However, as shown in our previous work [7], the distribution of BOLD signals within an ROI is also *spatially* modulated by task. Thus, analyzing connectivity with spatial features may elucidate brain networks that are undetected by mean intensity measures.

In this paper, we propose characterizing the modulations in spatial variance of BOLD signals within different ROIs to infer functional connectivity between brain regions. To identify the functional networks in the brain, we employ replicator dynamics, which has previously been applied to functional neuroimaging by Lohmann and Bohn [8] as well as Neurmann et al. [9, 10]. Replicator dynamics is a well known concept that originated from theoretical biology for modeling the evolution of self-replicating interacting species, where each species is associated with a fitness value, and only the fittest species survives over time [11]. In the present context, brain regions play the role of interacting species and the correlation between the regions is the fitness. Thereby, applying replicator dynamics will find the brain regions that exhibit the highest degree of covariance. We note an important property of replicator dynamics is that it ensures each ROI within a detected network is closely connected to *all* other ROIs in the network, which is not guaranteed by methods like clustering or PCA [10].

2. MATERIALS

After obtaining informed consent, fMRI data were collected from 10 healthy subjects performing a right-handed motor task that involved squeezing a bulb with sufficient pressure such that a black horizontal bar shown on a screen was kept within an undulating pathway (Fig. 1(a)).

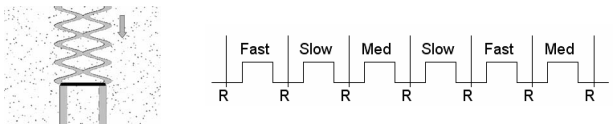

(a) (b)

Fig. 1. Experimental task and stimulus timing. (a) Subjects were required to keep the side of the black bar on the gray path. (b) R = rest, Slow, Med, and Fast = stimulus at 0.25, 0.5, and 0.75 Hz.

The pathway remains straight during rest periods and becomes sinusoidal with a frequency of 0.25 Hz (slow), 0.5 Hz (medium) or 0.75 Hz (fast) at time of stimulus. Each run lasted 260 s, consisting of a 20 s rest period at the beginning and end, 6 stimuli of 20 s duration in the order shown in Fig. 1(b), and a 20 s rest period between the stimuli.

2.1. fMRI data acquisition

Functional MRI was performed on a Philips Gyroscan Intera 3.0 T scanner (Philips, Best, Netherlands) equipped with a head-coil. We collected echo-planar (EPI) T2*-weighted images with BOLD contrast. Scanning parameters were: repetition time 1985 ms, echo time 3.7 ms, flip angle 90°, field of view (FOV) 216×143×240 mm, in plane resolution 128×128 pixels, pixel size 1.9×1.9 mm. Each functional run lasted 4 minutes where 36 axial slices of 3 mm thickness were collected in each volume, with a gap thickness of 1 mm. We selected slices to cover the dorsal surface of the brain and included the cerebellum ventrally. A high resolution three dimensional (3D) T1-weighted image consisting of 170 axial slices was acquired for the whole brain to facilitate anatomical localization of activation.

2.2. fMRI preprocessing

The acquired fMRI data was preprocessed for each subject, using Brain Voyager's (Brain Innovation B.V.) trilinear interpolation for 3D motion correction and sinc interpolation for slice time correction. Further motion correction was performed using motion corrected independent component analysis (MCICA) [12]. To correct for temporal autocorrelations, each voxel's intensity time course was high-pass filtered at 0.02 Hz (paradigm frequency being 0.025 Hz) with the residual autocorrelations modeled as an autoregressive AR(1) process, as in SPM2 [1]. We note that *no* spatial warping and smoothing were performed.

The Brain Extraction Tool (BET) in MRIcro [13] was used to strip off the skull of the anatomical and first functional image volume in each run to enable more accurate alignment of the functional and anatomical scans. Custom scripts to co-register the anatomical and functional images were generated using the Amira software (Mercury Computer Systems, San Diego, USA).

Sixteen motor-related ROIs were manually drawn on each unwarped structural scan using Amira. The ROIs were drawn separately in each hemisphere, based upon anatomical landmarks and guided by a neurological atlas [14]. ROIs included: putamen, caudate, thalamus, cerebellum, primary motor cortex (M1), supplementary motor area (SMA), prefrontal cortex (PFC), and anterior cingulated cortex (ACC). The labels on the segmented anatomical scans were resliced at the fMRI resolution. The raw time courses of the voxels within each ROI were then extracted for analysis.

3. METHODS

Our proposed network detection framework involves first extracting a spatial feature time course from the BOLD signal within each ROI. Pairwise correlations between the ROI spatial feature time courses are then calculated after which replicator dynamics [8] is applied to the mean correlation matrix (averaged over subjects) to identify brain networks that are common across subjects.

3.1. BOLD spatial feature time courses

In our previous work [7], we used 3D moment descriptors to characterize the spatial modulation of BOLD signals within an ROI, and demonstrated that such modulation is not random, but in fact task-related. In this paper, we are extending the application of 3D moment descriptors to examine functional connectivity between brain regions. 3D moment descriptors are based on centralized 3D moments:

$$\mu_{pqr}(t) = \int_{-\infty}^{\infty}\int_{-\infty}^{\infty}\int_{-\infty}^{\infty}(x-\bar{x})^p(y-\bar{y})^q(z-\bar{z})^r\rho(x,y,z,t)dxdydz \quad (1)$$

where $p + q + r$ is the order of the moment, (x,y,z) are the coordinates of a voxel, $\rho(x,y,z,t)$ is the intensity of a voxel located at (x,y,z) inside a given ROI at time t, and $\bar{x}$, $\bar{y}$, and $\bar{z}$ are the centroid coordinates of $\rho(x,y,z,t)$. To untangle the effect of amplitude changes, $\rho(x,y,z,t)$ is normalized such that the intensity values of the voxels within the ROI sum up to one at every time point t. This step ensures that the mean ROI intensity does not change with time. Thus, any detected modulations in the spatial feature will be purely due to spatial changes in the BOLD signal. In this study, we focused on a single 2nd order 3D moment descriptor that characterizes spatial variance [15]:

$$J_1(t) = \mu_{200}(t) + \mu_{020}(t) + \mu_{002}(t) \quad (2)$$

To compare with the results obtained using $J_1(t)$, the traditionally used mean intensity time courses, $I(t)$, for each ROI of a given subject is also calculated by averaging the unnormalized intensities within the ROI at every time point.

3.2. Connectivity inference using replicator dynamics

The basic principle of replicator dynamics is as follows. Let W be a matrix with elements w_{ij} corresponding to the similarity between ROI_i and ROI_j. w_{ii} is set to zero to avoid self connections and w_{ij} can be any similarity measure such as Spearman's correlation, as used in this study and in [8] for its robustness to the different possible probability distributions of the ROI features [16]. Let x be a vector with x_i representing the degree of membership of ROI_i belonging to the maximally correlated network (often referred to as the dominant network). Replicator dynamics finds the vector x that maximizes x^TWx with the constraints of $x_i \geq 0$ and $\sum x_i = 1$ by iteratively applying (3):

$$x_i(k+1) = x_i(k)\frac{(Wx(k))_i}{x(k)^TWx(k)} \tag{3}$$

where k is the iteration number and $x_i(0)$ is initialized to $1/N$ (N = number of ROIs) so that all ROIs have equal chances of being in the dominant network at the beginning of the optimization to avoid any bias. Based on the fundamental theorem of natural selection [11], $x_i(k)$ is guaranteed to converge to a local maximum, where x_i's associated with those ROIs that belong to the dominant network will increase above $1/N$, while other x_i's will decrease below $1/N$. Therefore, after x stabilizes, the ROIs corresponding to $x_i > 1/N$ are declared members of the dominant network. To detect subsequent networks of lower correlation, one can remove the ROIs belonging to the previously detected networks and repeat the procedures above [8].

For making group inferences, we need to average the w_{ij}'s across subjects. However, since our chosen w_{ij} does not follow a normal distribution, we convert the w_{ij}'s to z_{ij} using Fisher's z-transform, which is approximately normal [16]:

$$z_{ij} = 0.5\ln\left(\frac{1+w_{ij}}{1-w_{ij}}\right) \tag{4}$$

The resulting z_{ij}'s are then averaged across subjects, and the average w_{ij}'s can be obtained by applying the inverse Fisher's z-transform to the average z_{ij}'s:

$$w_{ij} = \frac{\exp(2z_{ij})-1}{\exp(2z_{ij})+1} \tag{5}$$

The above algorithm provides a simple means for identifying functional networks, but a minor drawback is that given any arbitrary W, replicator dynamics will still be able to find a network. Therefore, we applied replicator dynamics to 10,000 sets of randomly generated Gaussian signals, and determined the maximum value of x^TWx to be approximately 0.2, above which the detected networks are not likely to be artificial. In this paper, all dominant networks presented have x^TWx exceeding 0.2.

4. RESULTS AND DISCUSSION

In this work, we are interested in comparing the networks detected using our recently proposed measures of fMRI spatial modulation with traditional mean intensity measures as ROI features. Also, we investigated whether, and if so how, the composition of the functional networks changes with task frequency. The ROI feature time courses were first divided into segments based on task frequency as shown in Fig. 1(b). Time course segments corresponding to the same task frequency were then concatenated.

Fig. 2 summarizes the results obtained by applying replicator dynamics to the different segments of ROI feature time courses. Figs. 2(a-c) correspond to slow, medium, and fast frequency results obtained with our proposed spatial variance time courses $J_1(t)$. At slow frequency, the left and right PFCs were detected as the dominant network with the SMAs being the second most dominant network and the ACCs being the third most dominant network. Observing regions from the left side of the brain connected to the same anatomical structure on the right is not too surprising, since they are physically connected through the corpus callosum. As we increased the task frequency from slow to medium, the left cerebellum, which is part of the ipsilateral cortico-cerebellar-thalamic loop, was additionally recruited. At the fastest frequency, the right SMA became part of the dominant network, and the right cerebellum and the left and right caudate nuclei were further recruited. The right cerebellum is known to be related to visually-guided movements and the caudate nuclei are responsible for timing of motor movements. Thus, observing recruitments of these ROIs at higher frequencies conforms to prior neuroscience knowledge. In contrast, Figs. 2(d-f) correspond to the results obtained with mean ROI intensity time courses. In general, except for the third most dominant network, no frequency related changes were detected using mean intensity. Considering only the third most dominant network, both the left and right caudate nuclei and the thalami were recruited at slow frequency, and the caudate nuclei appeared to be replaced by the right M1 at medium frequency. At fast frequency, the thalami and right M1 were no longer part of the network as replaced by the caudate nuclei and left putamen, which were members of the slow frequency network. These results are rather intriguing, since one would expect a gradual change in network composition with increasing task frequency. To determine the source of these unexpected results, we examined the fourth most dominant network and found the bilateral putamen to be in the slow frequency network, the caudate nuclei in the medium frequency network, and the thalami and right M1 in the fast frequency network. Thus, if we consider the union of the third and fourth most dominant networks (which had comparable degree of correlation), very similar networks were in fact detected for all frequencies with mean intensity. Hence, spatial modulation appears to be a more sensitive ROI feature for detecting frequency related network changes, which suggests that functional connectivity is not simply governed by intensity changes as traditionally believed.

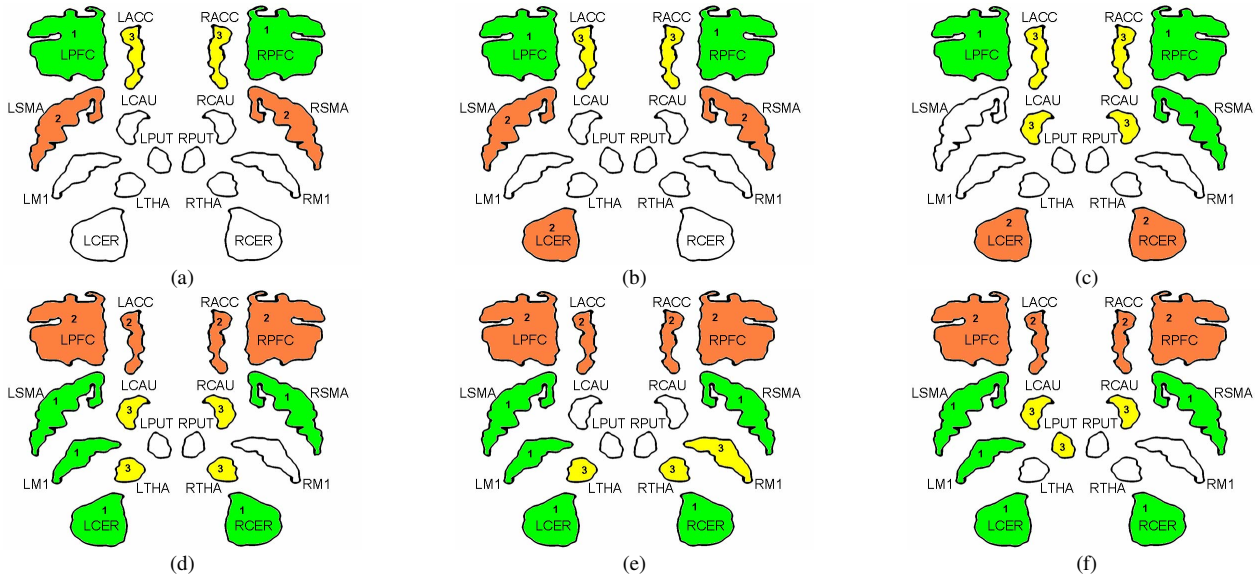

Fig. 2. Functional network detection with replicator dynamics. PUT = putamen, CAU = caudate, THA = thalamus, CER = cerebellum. The first and second rows correspond to using spatial variance and mean intensity as ROI features, respectively. The columns correspond to slow, medium, and fast frequencies. The level of correlation of the detected networks is coded by colour and number with ROIs in green-1 being the most correlated, in orange-2 being second most correlated, and in yellow-3 being third most correlated. Spatial variance appears to be a more sensitive feature for detecting frequency related network composition changes than mean intensity.

5. CONCLUSIONS

In this paper, we demonstrated, for the first time, that spatial modulation of BOLD signals within distinct ROIs can be effectively used to infer functional connectivity from fMRI data. By applying replicator dynamics to our recently proposed fMRI spatial feature time courses, we were able to detect frequency related changes in the composition of the functional networks, whereas little changes were observed with intensity measures. A direct extension would be to examine effective connectivity with the proposed spatial features, an approach currently being pursued.

6. REFERENCES

[1] R. S. J. Frackowiak, K. J. Friston, C. Frith, R. Dolan, C. J. Price, S. Zeki, J. Ashburner, and W. D. Penny, *Human Brain Function*, 2nd ed., Academic Press, 2003.

[2] K. J. Friston, C. D. Frith, P. F. Liddle, and R. S. Frackowiak, "Functional connectivity: the principal-component analysis of large (PET) data sets," *J. Cereb. Blood Flow Metab.,* vol. 13, pp. 5-14, 1993.

[3] K. J. Friston, C. Buechel, G. R. Fink, J. Morris, E. Rolls, and R. J. Dolan, "Psychophysiological and Modulatory Interactions in Neuroimaging," *Neuroimage,* vol. 6, pp. 218-229, 1997.

[4] B. Biswal, F. Z. Yetkin, V. M. Haughton, and J. S. Hyde, "Functional connectivity in the motor cortex of resting human brain using echo-planar MRI," *Magn. Reson. Med.,* vol. 34, pp. 537-541, 1995.

[5] A. Nieto-Castanon, S. S. Ghosh, J. A. Tourville, and F. H. Guenther, "Region of interest based analysis of functional imaging data," *Neuroimage,* vol. 19, pp. 1303–1316, 2003.

[6] Y. Liu, J. H. Gao, M. Liotti, Y. Pu and P. T. Fox, "Temporal dissociation of parallel processing in the human subcortical outputs," *Nature,* vol. 400, pp. 364-367, 1999.

[7] B. Ng, R. Abugharbieh, S. J. Palmer, and M. J. McKeown, "Characterizing task-related temporal dynamics of spatial activation distributions in fMRI BOLD signals," *MICCAI 2007*, Part I, LNCS 4791, pp. 767-774, 2007.

[8] G. Lohmann and S. Bohn, "Using replicator dynamics for analyzing fMRI data of the human brain," *IEEE Trans. Med. Imaging,* vol. 21, pp. 485-492, 2002.

[9] J. Neumann, G. Lohmann, J. Derrfuss, and D. Y. von Cramon, "Meta-analysis of functional imaging data using replicator dynamics," *Hum. Brain Mapp.,* vol. 25, pp. 165-173, 2005.

[10] J. Neumann, D. Y. von Cramon, B. U. Forstmann, S. Zysset, and G. Lohmann, "The parcellation of cortical areas using replicator dynamics in fMRI," *Neuroimage,* vol. 32, pp. 208-219, 2006.

[11] P. Schuster and K. Sigmund, "Replicator dynamics," *J. Theor. Biol.,* vol. 100, pp. 533-538, 1983.

[12] R. Liao, J. L. Krolik, and M. J. McKeown, "An information-theoretic criterion for intrasubject alignment of FMRI time series: motion corrected independent component analysis," *IEEE Trans. Med. Imaging,* vol. 24, pp. 29-44, 2005.

[13] C. Rorden and M. Brett, "Stereotaxic display of brain lesions," *Behav. Neurol.,* vol. 12, pp. 191-200, 2000.

[14] J. Talairach and P. Tournoux, *Co-Planar Stereotaxic Atlas of the Human Brain: 3-Dimensional Proportional System: An Approach to Cerebral Imaging,* Thieme, 1988.

[15] F. A. Sadjadi and E. L. Hall, "Three-dimensional moment invariants," *IEEE Trans. Pattern Anal. Mach. Intell.,* vol. 2, pp. 127-136, 1980.

[16] B. P. Flannery, W. H. Press, S. A. Teukolsky and W. T. Vetterling, "Numerical Recipes in C," *Press Syndicate of the University of Cambridge, New York,* 1992.